Life Sciences 216 (2019) 129–139

Contents lists available at ScienceDirect

Life Sciences

journal homepage: www.elsevier.com/locate/lifescie

Loss of pigment epithelium-derived factor leads to ovarian oxidative damage accompanied by diminished ovarian reserve in mice

Xing-hui Li[a,b,c], Hai-ping Wang[a,b,c], Jing Tan[a,b,c], Yan-di Wu[a,b,c], Ming Yang[a,b,c], Cheng-zhou Mao[a,c], Sai-fei Gao[a,c], Hui Li[a,c], Hui Chen[d,*], Wei-bin Cai[a,b,c,e,**]

[a] Guangdong Engineering & Technology Research Center for Disease-Model Animals, Program in Cardiovascular Disease and Metabolism, the Fifth Affiliated Hospital, Zhongshan School of Medicine, Sun Yat-sen University, Guangzhou 510080, Guangdong Province, China
[b] Department of Biochemistry, Zhongshan Medical School, Sun Yat-sen University, Guangzhou 510080, Guangdong Province, China
[c] Laboratary Animal Center, Sun Yat-sen University, Guangzhou 510080, Guangdong Province, China
[d] Department of Obstetrics and Gynecology, Sun Yat-sen Memorial Hospital, Sun Yat-sen University, Guangzhou 510120, Guangdong Province, China
[e] The Key Laboratory for Stem Cells and Tissue Engineering, Ministry of Education, Sun Yat-Sen University, Guangzhou 510080, Guangdong Province, China

ARTICLE INFO

Keywords:
Pigment epithelium-derived factor
Ovarian oxidative damage
Diminished ovarian reserve
Insulin resistance
Lipotoxicity

ABSTRACT

Aims: This study aims to investigate the pathophysiological role and mechanism of pigment epithelium-derived factor (PEDF) deletion in ovarian damage.

Methods: Female PEDF-knockout mice and their wild-type littermates were used in this study. Relevant tests were performed at 8–10 weeks or 32 weeks of age.

Key findings: Compared to the wild-type mice, the PEDF-knockout mice showed diminished ovarian reserve (DOR), worse ovum quality after injection to induce controlled ovarian stimulation, increased serum follicle stimulating hormone (FSH) level and an follicle stimulating hormone/luteinizing hormone (FSH/LH) ratio. Moreover, severe ovarian oxidative damage was found in ovaries of PEDF-knockout mice that mainly manifested as an accumulation of reactive oxygen species (ROS), NF-E2-related factor 2 (Nrf2) pathway activation, significantly upregulated expression of ROS-generating genes. Correspondingly, the PEDF-knockout mice exhibited lipid metabolism disorder and insulin resistance, which mainly manifested as obesity, abdominal fat accumulation, adipocyte enlargement, severe ectopic fat deposition, dyslipidemia, changes in adipokine levels, hyperglycemia, hyperinsulinemia, impaired glucose tolerance, impaired insulin tolerance and significantly declined protein kinase B (Akt) phosphorylation levels.

Significance: Loss of PEDF leads to ovarian oxidative damage accompanied by DOR in mice, this is related to PEDF deficiency induced severe insulin resistance and lipid metabolism disorder. Therefore, PEDF may be a potential target for the treatment of diseases related to ovarian oxidative damage.

1. Introduction

The ovary has important physiological functions, including ovulation and endocrine roles [1]. Impaired ovarian function severely affects women's reproductive health and is an important factor in female infertility [1–3]. Destruction of the body's antioxidant system results in the accumulation of large amounts of reactive oxygen species (ROS) in tissues and ultimately in oxidative stress, which impairs tissue functions. Ovarian oxidative damage can lead to severe ovarian dysfunction and multiple diseases, such as polycystic ovary syndrome (PCOS), decreased ovarian reserve (DOR), and premature ovarian failure [1,3–5].

Pigment epithelium-derived factor (PEDF) is a secreted protein with a molecular weight of 50 kD that consists of 418 amino acids, which is located at 17p13.1, contains 8 exons and 7 introns [6]. Although PEDF is a member of the serine protease superfamily, it does not possess the protease inhibition function [7]. PEDF is widely distributed in human tissues, including the liver, fat, ovary, heart, kidney, and skeletal muscle [8–10]. As a multi-functional protein, PEDF has a powerful function of inhibiting angiogenesis, and it can inhibit the formation of

* Correspondence to: H. Chen, Department of Obstetrics and Gynecology, Sun Yat-sen Memorial Hospital, Sun Yat-sen University, No.74 Yanjiang West Road, Guangzhou 510120, Guangdong Province, China.
** Correspondence to: W.-b. Cai, Department of Biochemistry, Zhongshan Medical School, Sun Yat-sen University, No.74 Zhongshan Road II, Guangzhou 510080, Guangdong Province, China.
E-mail addresses: chenhui9@mail.sysu.edu.cn (H. Chen), caiwb@mail.sysu.edu.cn (W.-b. Cai).

https://doi.org/10.1016/j.lfs.2018.11.015
Received 28 September 2018; Received in revised form 26 October 2018; Accepted 6 November 2018
Available online 07 November 2018
0024-3205/ © 2018 Elsevier Inc. All rights reserved.

atherosclerotic plaque by anti-oxidation in endothelial cells, and can protect motor neurons from chronic glutamate-mediated neurodegeneration [10–12]. Additionally, although previous studies have confirmed that PEDF is closely related to insulin resistance, whether PEDF contributes to insulin sensitivity or leads to insulin resistance is a source of controversy [10,13–15]. In addition, an increasing number of studies have focused on the function of PEDF in regulating lipid metabolism. Clinical research data showed that circulating PEDF levels were significantly higher in patients with obesity, metabolic syndrome, diabetes and PCOS than in the normal population; the PEDF concentration was also positively correlated with triglyceride (TG) and negatively correlated with high-density lipoprotein (HDL) [16–21]. Nevertheless, it is still controversial whether the elevation of PEDF level leads to the occurrence of metabolic diseases or the compensatory elevation of PEDF level caused by metabolic diseases. Importantly, PEDF has been reported to have a significant anti-oxidative effect in a variety of cells, including granulosa cells [22–26]. However, whether PEDF deficiency can induce ovarian damage in mice and whether its role is related to oxidative stress, lipid metabolism disorders and insulin resistance remains unknown. To test this hypothesis, we used PEDF-knockout mice to investigate the effect of PEDF on ovarian damage.

2. Materials and methods

2.1. Reagents

Pregnant mare serum gonadotrophin (PMSG) and human chorionic gonadotropin (HCG) were obtained from Ningbo Second Hormone Factory (Ningbo, Zhejiang, China). Dihydroethidium (DHE) was obtained from Beyotime Biotechnology Co., Ltd. (Shanghai, China). Oil red O was obtained from Sigma-Aldrich (St. Louis, MO, USA). Mouse follicle stimulating hormone (FSH) and luteinizing hormone (LH) enzyme-linked immunosorbent assay kits were obtained from Xinle Biotechnology Co., Ltd. (Shanghai, China). Mouse insulin enzyme-linked immunosorbent assay kit was obtained from Cusabio Biotechnology Co., Ltd. (Wuhan, Hubei, China). Mouse adiponectin and leptin enzyme-linked immunosorbent assay kits were obtained from R&D Systems (Minnesota, USA). Other reagents information is presented in the corresponding methods section.

2.2. Animals and treatment

PEDF (−/−) mice on a C57BL/6J background were provided by Dr. Guoquan Gao (Zhongshan School of Medicine, Sun Yat-sen University) following breeding and expansion of a population from the Center for Disease Model Animals of Sun Yat-sen University. Female PEDF (−/−) mice and their wild-type littermates were used in this study. All animals were kept under 12-h light-dark cycles at 20–22 °C with free access to water and standard chow. The period of the primary experiment lasted from the birth of the animals to the 32nd week of life (6 animals per group). Glucose and insulin tolerance tests were performed at the 30th and 31st week. Gross photographs and micro-CT images were taken at the 32nd week. Then, the animals were sacrificed after 12–16 h of fasting, and sera and tissues were collected for subsequent testing. To avoid the chance of artificially induced cornification of the vaginal epithelium, the stage of the estrous cycle were identified by the appearance of the vagina as previously described at the end of the experiment [27]. In this study, as the vaginas of animals were gaping and the tissues were reddish-pink and moist, numerous longitudinal folds or striations were visible on both the dorsal and ventral lips at the end point, the animals were confirmed that they were in the proestrum stage of the estrous cycle. 12 ovaries were collected in each group, six ovaries from six individual mice were used for tissue section (three ovaries for paraffin section and another three ovaries for frozen section) and another six ovaries from six individual mice for other molecular biology tests (three ovaries for protein expression analysis and another three ovaries for mRNA level analysis). In the controlled ovarian stimulation experiment, female PEDF (−/−) mice and their wild-type littermates were used at 8–10 weeks of age (3 animals per group). All studies involving animal experimentation were approved by the Animal Care and Ethics Committee of Sun Yat-sen University and followed the National Institutes of Health Guidelines on the Care and Use of Animals.

2.3. DHE staining

The ovaries were fixed in 4% paraformaldehyde for 24 h, dehydrated with a sucrose gradient, and embedded in the Tissue-Tek OCT compound (Sakura Finetek, Tokyo, Japan). Then, the sections (5 μm) were stained with DHE following incubation at 37 °C for 30 min. The fluorescence intensity was quantified from three individual mice and five fields per mouse with the ImageJ software program (National Institutes of Health, Bethesda, MD, USA).

2.4. Hematoxylin and eosin (HE) staining

The ovaries and adipose tissues were fixed in 4% paraformaldehyde for 24 h, and serially sectioned (5 μm). Every third section (15 μm) was stained with HE for morphometric analysis as previously described [28]. The sizes (area) of the ovum were quantified based on HE staining in the maximum surface of the slice from three individual mice with the ImageJ software program (National Institutes of Health, Bethesda, MD, USA). In terms of follicular counts, only follicles where the oocyte nucleus could be identified were counted to avoid repeat counts of the same follicle based on the serially sections. Ovarian follicles were classified as primordial (single layer of flattened granulosa cells), primary (single layer of cuboidal or mixed cuboidal/flattened granulosa cells), secondary (greater than one layer of granulosa cells), or antral (possessing an antral cavity or several fluid filled vesicles in the case of early antral follicles) as previously described [4]. The sizes of the adipocytes were quantified based on HE staining in the maximum surface of the slice from three individual mice and five fields per mouse with the ImageJ software program (National Institutes of Health, Bethesda, MD, USA).

2.5. Controlled ovarian stimulation

Female PEDF (−/−) mice and their wild-type littermates (3 animals per group) at 8–10 weeks of age were superovulated with an intraperitoneal injection of 7.5 IU of PMSG at 17:00, followed by an additional injection of 7.5 IU of HCG 48 h later. The ovulated oocytes in the two oviducts of each mouse were collected and counted after 16 h. Oocytes with disordered cytoplasm, a large number of coarse grains in the central region, rough surface, deep overall coloration, or fragmentation, or large perivitelline space, were defined as low-quality oocytes. The numbers of oocytes and the low-quality oocytes were calculated, the sizes of oocytes were quantified with the ImageJ software program (National Institutes of Health, Bethesda, MD, USA).

2.6. Serum measurement

Sera (6 samples per group) were obtained by centrifugation of clotted blood collected from the eye sockets of the mice and stored at −80 °C. The serum FSH, LH, fasting insulin levels (FINS), adiponectin and leptin levels were examined using an enzyme-linked immunosorbent assay. The serum total cholesterol (TC), TG, free fatty acids (FFAs), HDL and low-density lipoprotein (LDL) levels were examined using commercial reagent kits (Jiancheng, Nanjing, Jiangsu, China).

2.7. Microcomputed tomography (micro-CT) imaging

Mice (3 animals per group) were anesthetized with an

intraperitoneal injection of 80 mg/kg of sodium pentobarbital and then subjected to micro-CT using the Siemens Inveon PET/CT scanner (Siemens Medical Solutions, Knoxville, TN, USA) with the mice in a supine position to assess body fat accumulation.

2.8. Oil red O staining

The livers and ovaries were fixed in 4% paraformaldehyde for 24 h, dehydrated with a sucrose gradient, and embedded in the Tissue-Tek OCT compound (Sakura Finetek, Tokyo, Japan). Then, the sections (5 μm) were stained with oil red O for 10 min. The positive area was quantified based on oil red O staining from three individual mice and five fields per mouse with the ImageJ software program (National Institutes of Health, Bethesda, MD, USA).

2.9. Glucose tolerance test (GTT) and insulin tolerance test (ITT)

The fasting blood glucose (FBG) levels were examined after the mice had fasted for 12–16 h using a glucometer (One Touch Ultra Easy, Life Scan, Wayne, PA, USA), and the homeostasis model assessment-insulin resistance (HOMA-IR) was calculated with the equation (FBG(mmol/L) ∗ FINS(mIU/L))/22.5. To perform the glucose tolerance tests, 1 g/kg of glucose (Sigma-Aldrich, St. Louis, MO, USA) was i.p. injected into the mice, whereas 1 U/kg of insulin (Novolin R, Novo Nordisk, Bagsvaerd, Denmark) was i.p. injected into the mice for the insulin tolerance test. The blood glucose levels were examined 0, 15, 30, 60 and 120 min after the injection. The change curve of the blood glucose level was drawn, and the area under the curve (AUC) was calculated (6 animals per group).

2.10. Immunohistochemistry (IHC)

The ovaries (3 samples per group) were fixed in 4% paraformaldehyde for 24 h, dehydrated with a sucrose gradient, and embedded in the Tissue-Tek OCT compound (Sakura Finetek, Tokyo, Japan). Then, the sections (5 μm) were blocked with 3% hydrogen peroxide and then performed at 95 °C for 10 min using citrate buffer (Beyotime, Shanghai, China), then blocking steps were carried out using the QuickBlock™ Blocking Buffer (Beyotime, Shanghai, China) according to the manufacturer's instructions. After incubated with primary antibody for superoxide dismutase 1 (SOD1) (GB11263, 1:500 dilution, Servicebio, Wuhan, Hubei, China) at 4 °C overnight, the sections incubated with secondary antibody (G1210, 1:250 dilution, Servicebio, Wuhan, Hubei, China) at 37 °C for 30 min. Visualization was accomplished using 3,-*N*-diaminobenzidine tertrahydrochloride (Beyotime, Shanghai, China). Sections were counterstained with hematoxylin (Servicebio, Wuhan, Hubei, China). The mean density was quantified from three individual mice and five fields per mouse with the ImageJ software program (National Institutes of Health, Bethesda, MD, USA).

2.11. Quantitative real-time polymerase chain reaction (Q-PCR)

Total RNA was isolated from the ovarian tissues (3 samples per group) using the RNeasy Mini Kits according to the manufacturer's instruction (Qiagen, Hilden, Germany). Two micrograms of total RNA was reverse transcribed into complementary DNA in a 20-μl reaction mixture using the ImProm-II™ Reverse Transcription System (Promega, Madison, WI, USA). The Q-PCR was performed using the SYBR Green PCR Master Mix and the ABI Prism 7500 Real-Time PCR machine (Applied Biosystems, Foster City, CA, USA). The relative gene expression levels were analyzed using the 2(–ΔΔCt) method and normalized against β-actin expression. The following primer sequences were used: acyl-coenzyme A oxidase (Aco) forward 5′-TGGTATGGTGTCGTACTT GAATGAC-3′ and reverse 5′-AATTTCTACCAATCTGGCTGCAC-3′; cytochrome P450 2E1 (CYP2E1) forward 5′-TGTGACTTTGGCCGACCTG TTC-3′ and reverse 5′-CAACACACACGCGCTTTCCTGC-3′; NADPH oxidase-2 (Nox2) forward 5′-GAAAACTCCTTGGGTCAGCACT-3′ and reverse 5′-ATTTCGACACACTGGCAGCA-3′; and β-actin forward 5′-TACCACCATGTACCCAGGCA-3′ and reverse 5′-CTCAGGAGGAGCAAT GATCTTGAT-3′.

2.12. Western blotting analysis

The ovarian tissues (3 samples per group) were lysed with RIPA buffer (Beyotime, Shanghai, China) for total protein extraction. Nuclear proteins were extracted using a nuclear protein extraction kit (Beyotime, Shanghai, China). The protein concentration was determined using the BCA protein assay kit (Millipore, Bedford, MA, USA) according to the manufacturer's protocol. Equal amounts of protein were subjected to SDS-PAGE for electrophoresis, transferred to 0.45-μm PVDF membranes (Millipore, Bedford, MA, USA), and immunoblotted with antibodies against sequestosome 1 (SQSTM1), Nrf2, Histone H3, heme oxygenase-1 (HO-1), NAD(P)H:quinone oxidoreductase 1(NQO1), p-Akt(Thr308), p-Akt(Ser473), protein kinase B (Akt) and GAPDH. Antibodies against SQSTM1 (88588S, 1:1000 dilution), Nrf2 (12721S, 1:1000 dilution), HO-1 (70081S, 1:1000 dilution), p-Akt (13038S and 4060S, 1:1000 dilution), Akt (4691S, 1:1000 dilution), Histone H3 (4499S, 1:1000 dilution) and GAPDH (5174S, 1:2000 dilution) were obtained from Cell Signaling Technology (Beverly, MA, USA). The antibody against NQO1 (ab28947, 1:1000 dilution) was obtained from Abcam (Cambridge, MA, USA). The bands were quantified using the ImageJ software program (National Institutes of Health, Bethesda, MD, USA).

2.13. Statistical analysis

All analyses were performed with the Statistical Package for Social Sciences version 19.0 (SPSS, Chicago. IL, USA). The data were expressed as the mean ± SD. Statistical significance was determined by Student's *t*-test. In all statistical comparisons, a p value < 0.05 was used to indicate a statistically significant difference.

3. Results

3.1. PEDF-knockout mice showed impaired ovarian structure and ovarian reserve

To investigate the effect of PEDF deficiency on the ovarian structure of the mice, macroscopic pictures of ovaries, ovary weight and HE staining were performed. Compared to the ovaries of the wild-type mice, the ovaries of the PEDF-knockout mice showed decreased ovary weight and ovary weight/body weight ratio. (Fig. 1A,B,C) Additionally, the HE staining results showed that more different developmental stages follicles were found in the ovaries of wild-type mice. (Fig. 1D) Moreover, the ovaries of PEDF-knockout mice showed a smaller size and less primordial follicles, primary follicles, secondary follicles, antral follicles and corpora lutea compared to the wild-type mice. (Fig. 1E,F) These results suggested that PEDF deletion may lead to ovarian structural damage and decreased reserve.

3.2. PEDF-knockout mice showed severe ovarian dysfunction

To investigate the effect of PEDF deficiency on the ovarian function of the mice, controlled ovarian stimulation and serum hormone testing were performed. Oocytes with disordered cytoplasm, a large number of coarse grains in the central region, rough surface, deep overall coloration, or fragmentation, or large perivitelline space, were defined as low-quality oocytes. Although the numbers of oocytes and the oocyte size had no obvious difference, compared to the ovaries of the wild-type mice, controlled ovarian stimulation resulted in production of more low-quality oocytes during ovulation in the PEDF-knockout mice. (Fig. 2A–E) Additionally, although the serum biochemical test results

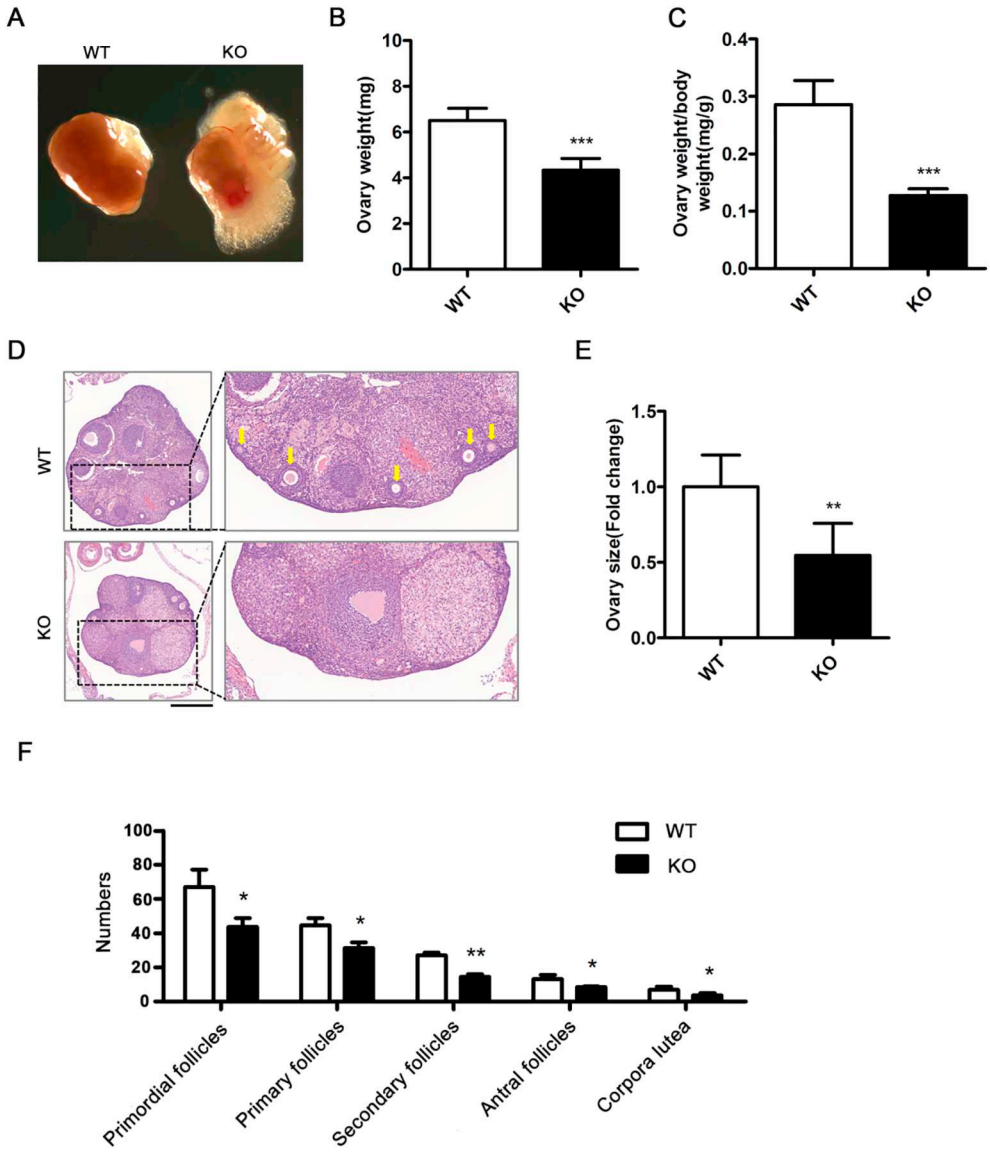

Fig. 1. PEDF-knockout mice showed impaired ovarian structure and ovarian reserve. A. Macroscopic pictures of ovaries. B. The ovaries weight. C. The ovary weight/body weight ratio. D. HE staining of ovarian tissues in the maximum surface of the slice (Scale bar = 500 μm, yellow arrows indicate follicles in different developmental stages). E. The ovary sizes (area) quantified based on the HE staining in the maximum surface of the slice. F. Numbers of different stage of follicles and corpora lutea quantified based on the HE staining of serially sections. Data are expressed as the mean ± SD. *, $p < 0.05$; **, $p < 0.01$; ***, $p < 0.001$. (For interpretation of the references to color in this figure legend, the reader is referred to the web version of this article.)

showed no difference in the serum LH levels between the PEDF-knockout and wild-type mice, the PEDF-knockout mice exhibited higher FSH levels and higher FSH/LH ratios. (Fig. 2F,G,H).

3.3. PEDF-knockout mice showed severe ovarian oxidative damage

To test the effect of PEDF deletion on oxidative stress in the mouse ovary, we performed DHE staining and evaluated the expression levels of the relevant proteins or mRNAs. We found that compared with the wild-type mice, the ovaries of the PEDF-knockout mice exhibited more ROS accumulation, whereas the mRNA expression levels of ROS-generating genes was significantly upregulated. (Fig. 3A,B) We also found that the expression of the antioxidant proteins SQSTM1, Nrf2, HO-1, NQO1 and SOD1 increased significantly in the ovaries of the PEDF-knockout mice. (Fig. 3C–F) The above results confirmed that the ovaries of the PEDF-knockout mice showed obvious oxidative stress.

3.4. Knockout of PEDF induced obesity phenotype

To observe the effect of PEDF on body weight, fat accumulation, abdominal adipose tissue weight, we performed the general photographs, weighing, micro-CT imaging and pathology tests. The PEDF-knockout mice developed an obese phenotype compared to the wild-type mice (Fig. 4A, B). The micro-CT imaging results confirmed that the PEDF-knockout mice exhibited more pronounced fat accumulation and increased abdominal adipose tissue weight than the wild-type mice (Fig. 4C,D). Furthermore, the adipocyte sizes of the PEDF-knockout mice were significantly larger than those of the wild-type mice (Fig. 4E,F). The above results demonstrated that the PEDF-knockout mice exhibit an obese phenotype.

3.5. Knockout of PEDF increased liver and ovarian ectopic fat deposition

To investigate the effect of PEDF deficiency on the ectopic fat deposition, oil red O staining were performed using the liver and ovarian tissues. The results showed that the liver and ovarian tissues of the PEDF-knockout mice showed more lipid accumulation than those of the wild-type mice (Fig. 5A–D). The above results demonstrated that the PEDF-knockout mice exhibit severe ectopic fat deposition.

3.6. Knockout of PEDF induced dyslipidemia and changed the circulating adipocytokine levels in the mice

To observe the effect of PEDF knockout on dyslipidemia in mice, we measured the serum lipid and adipocytokine levels. Significant disorder of lipid metabolism was observed in the PEDF-knockout mice, which

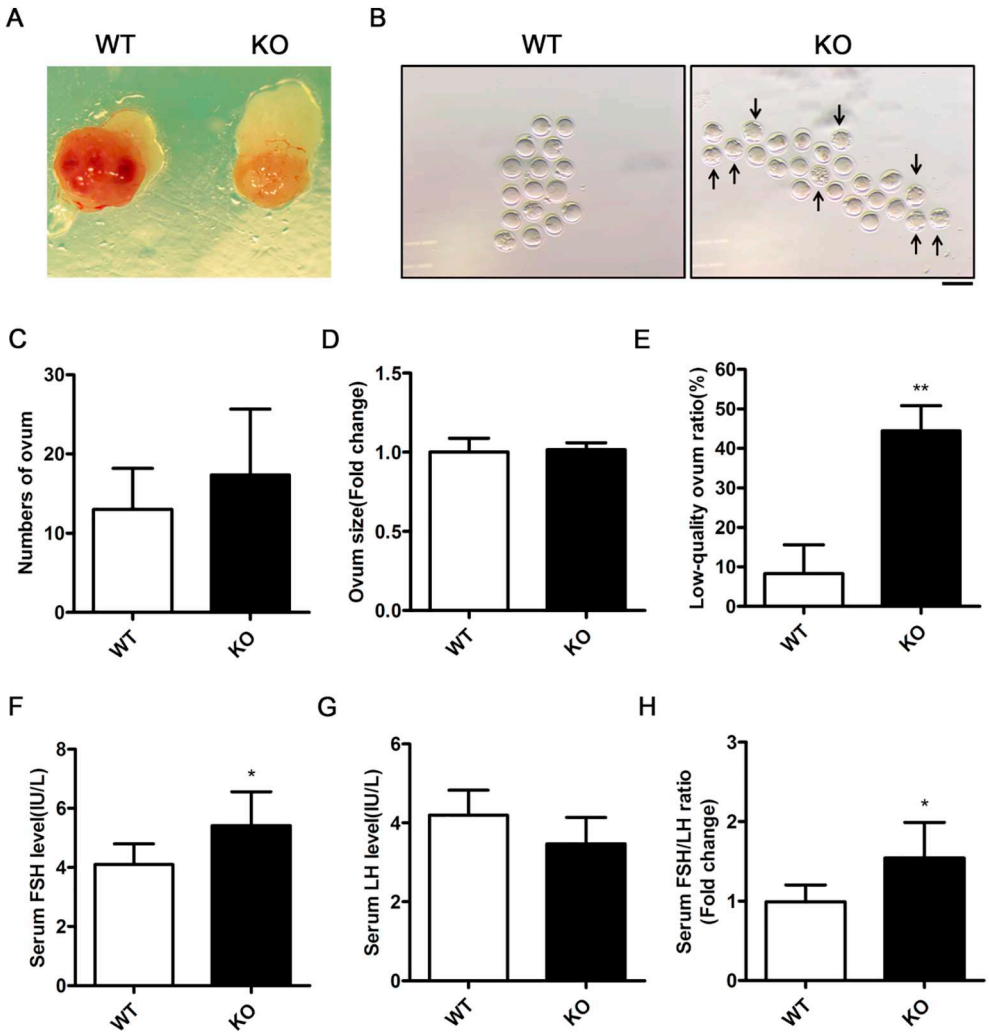

Fig. 2. PEDF-knockout mice showed severe ovarian dysfunction. A. Macroscopic pictures of ovaries after controlled ovarian stimulation. B. The oocytes collected from the mice after injection to induce controlled ovarian stimulation (Scale bar = 500 μm, black arrows indicate low-quality oocytes). C. Numbers of oocytes after controlled ovarian stimulation. D. Size of oocytes after controlled ovarian stimulation. E. Low-quality oocytes ratio after controlled ovarian stimulation. F. Sera FSH levels in the mice. G. Sera LH levels in the mice. H. Sera FSH/LH ratio in the mice. Data are expressed as the mean ± SD. *, $p < 0.05$; **, $p < 0.01$.

mainly manifested as elevated serum TC, TG, FFAs, and LDL levels, decreased HDL levels and a decreased HDL/LDL ratio (Fig. 6A–F). The serum adipocytokine levels also changed significantly in the PEDF-knockout mice. The serum adiponectin level was no change in the PEDF-knockout mice, but the leptin level was significantly increased, resulting in a significant decrease in the adiponectin/leptin ratio (Fig. 6G, H, I) The above results demonstrate the presence of a significant dyslipidemic disorder in the PEDF-knockout mice.

3.7. Knockout of PEDF increased the blood glucose level and induced hyperinsulinemia and insulin resistance

To investigate the effect of PEDF on glucose metabolism and insulin sensitivity, the serum glucose and insulin levels and tolerance were measured. We found that the PEDF-knockout mice showed higher FBG and FINS levels and a higher HOMA-IR than the wild-type mice (Fig. 7A, B, C). In addition, the ITT results showed that the PEDF-knockout mice had worse insulin sensitivity, which was mainly reflected in the smaller decrease in blood glucose and the slower rate of decline after insulin injection, resulting in a larger AUC (Fig. 7D). Correspondingly, the GTT showed that the PEDF-knockout mice had worse tolerance to glucose; for instance, the blood glucose of the PEDF-knockout mice reached its peak faster and the peak was higher than that of the wild-type mice after glucose injection, leading to a larger AUC (Fig. 7E). Additionally, as a downstream target of the insulin signaling pathway, Akt and its phosphorylation levels were also tested. The results showed that p-Akt(Thr308) and p-Akt(Ser473) expression was significantly decreased in the ovaries of the PEDF-knockout mice compared to the levels detected in the wild-type mice (Fig. 7F, G). The above results demonstrated that the PEDF-knockout mice exhibited significant insulin resistance, hyperglycemia, and hyperinsulinemia.

4. Discussion

In this study, we used PEDF-knockout mice and their wild-type littermates to investigate the effect of PEDF on ovarian oxidative damage and the corresponding mechanism. Loss of PEDF leads to ovarian oxidative damage accompanied by DOR in mice, this is related to PEDF deficiency induced severe insulin resistance and lipid metabolism disorder.

Under physiological conditions, follicles in different developmental stages are present in the ovary, and a fresh corpus luteum is produced after ovulation. In this study, smaller ovaries and less primordial follicles, primary follicles, secondary follicles, antral follicles and corpora lutea were found in the PEDF-knockout mice. Because ovarian oxidative stress can severely affect ovarian ovulation and reserve, controlled

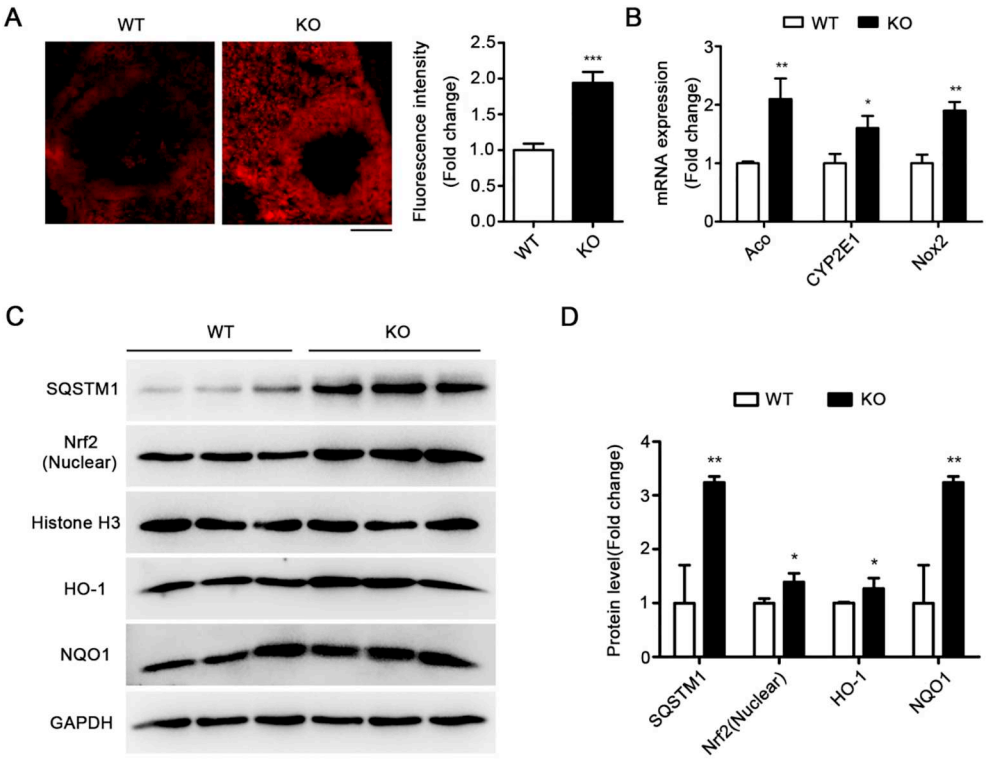

Fig. 3. PEDF-knockout mice showed ovarian oxidative damage. A. DHE staining of mouse ovaries (Scale bar = 100 μm) and the fluorescence intensity was quantified based on DHE staining of mouse ovaries. B. Fold changes of the mRNA expression levels of ROS-generating genes. C. The levels of SQSTM1/Nrf2 pathway proteins in mouse ovaries were detected by Western blotting. D. The fold changes of the protein levels related to the SQSTM1/Nrf2 pathway quantified based on the Western blotting results. E. The immunohistochemistry pictures of granulosa area SOD1 (Scale bar = 50 μm). F. The mean density of SOD1 based on the immunohistochemistry pictures. Data are expressed as the mean ± SD. *, $p < 0.05$; **, $p < 0.01$; ***, $p < 0.001$.

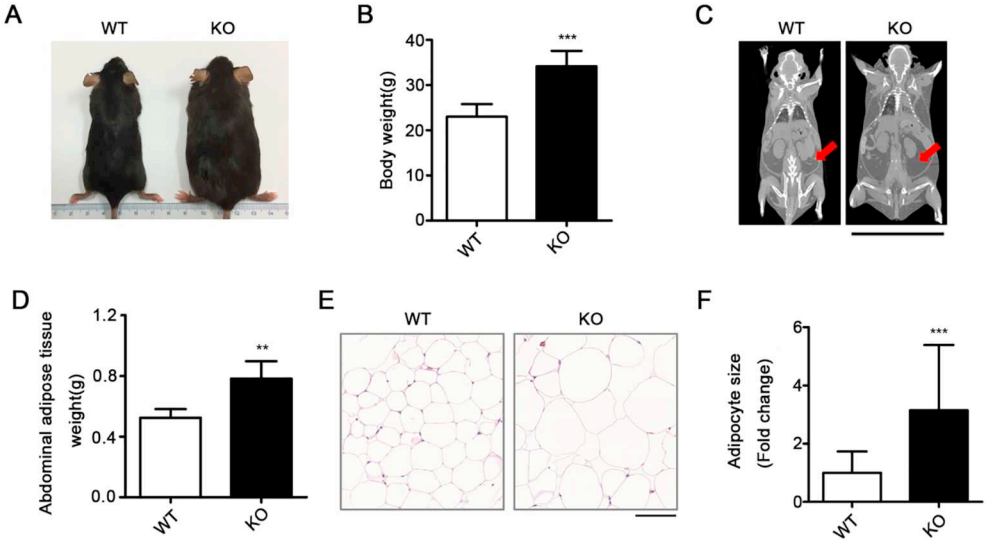

Fig. 4. Knockout of PEDF induced obesity phenotype. A. Macroscopic pictures of the mice. B. The body weights of the mice. C. Micro-CT imaging of the mice (Scale bar = 5 cm, a red arrow indicates abdominal fat). D. The abdominal adipose tissue weight. E. HE staining of abdominal adipocytes (Bar = 100 μm). F. The fold changes of size were quantified based on HE staining of adipocytes. Data are expressed as the mean ± SD. **, $p < 0.01$; ***, $p < 0.001$. (For interpretation of the references to color in this figure legend, the reader is referred to the web version of this article.)

ovarian stimulation and serum hormone testing were performed to clarify the impact of PEDF knockout on ovarian function. Compared to the wild-type mice, the PEDF-knockout mice showed a worse ovum quality after injection to induce controlled ovarian stimulation. Although there was no difference in the number of ovulation induction between PEDF-knock mice and the wild-type mice, which seems to be inconsistent with the diminished ovarian reserve of PEDF-knockout mice, we think this may be due to the smaller sample number in controlled ovarian stimulation, and the effect of PEDF deletion on ovulation induction sensitivity is unknown. Therefore, the above finding

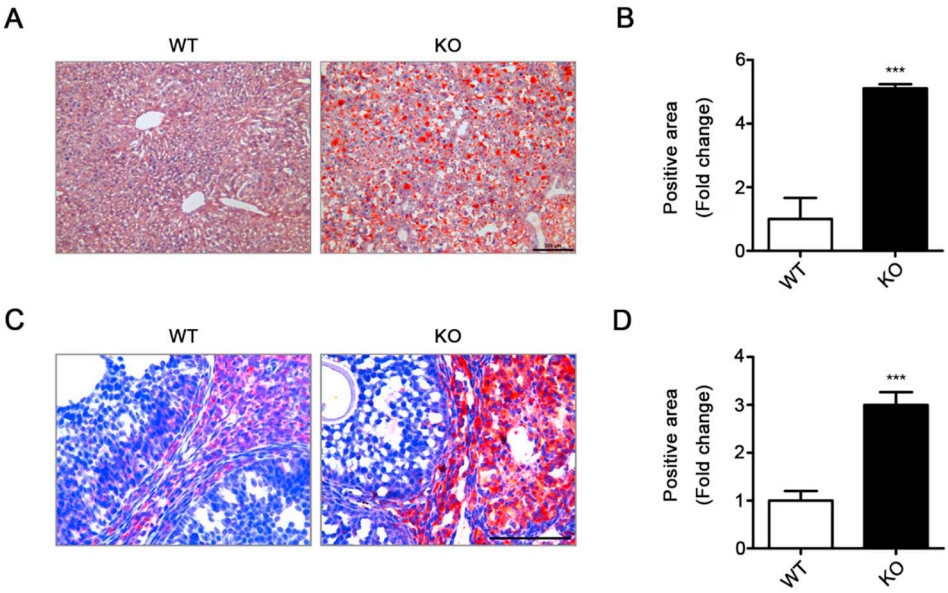

Fig. 5. Knockout of PEDF increased liver and ovarian ectopic fat deposition. A. HE staining of liver tissues (Scale bar = 200 μm). B. The fold changes of the positive areas were quantified based on oil red O staining of liver tissues. C. Oil red O staining of ovarian tissues (Scale bar = 100 μm). D. The fold changes of the positive areas were quantified based on oil red O staining of ovarian tissues. Data are expressed as the mean ± SD. ***, $p < 0.001$. (For interpretation of the references to color in this figure legend, the reader is referred to the web version of this article.)

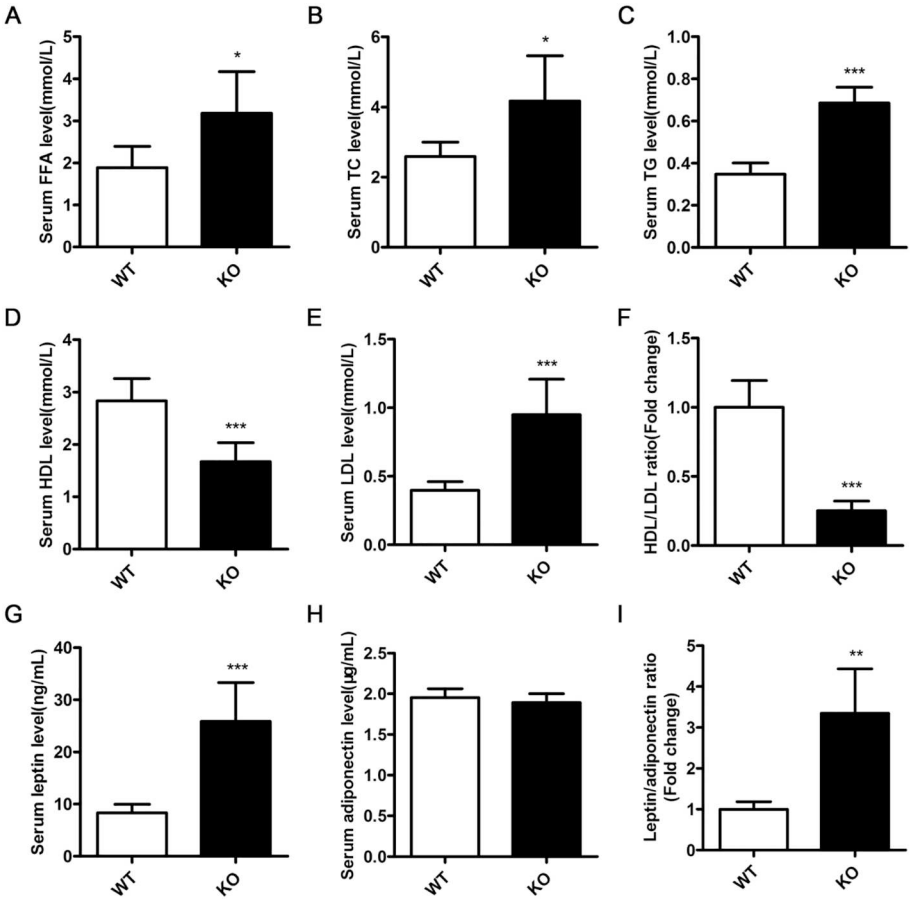

Fig. 6. Knockout of PEDF induced dyslipidemia and changed the circulating adipocytokine levels in mice. A. Sera FFA contents in the mice. B. Sera TC contents in the mice. C. Sera TG contents in the mice. D. Sera HDL contents in the mice. E. Sera LDL contents in the mice. F. Sera HDL/LDL ratios in the mice. G. Sera leptin levels in the mice. H. Sera adiponectin levels in the mice. I. Sera leptin/adiponectin ratios in the mice. Data are expressed as the mean ± SD. *, $p < 0.05$; **, $p < 0.01$; ***, $p < 0.001$.

suggested the occurrence of follicular developmental disorders in the PEDF-knockout mice. LH is a glycoprotein gonadotropin that is secreted by pituitary cells and promotes the conversion of cholesterol into sex hormones in gonadal cells. FSH is a hormone secreted by basophils in the anterior pituitary that regulates the body's development, growth, adolescent sexual maturity, and a series of physiological processes related to reproduction through stimulation of germ cell maturation. The FSH/LH ratio is considered an important indicator for evaluation of ovarian reserve function [29,30]. In this study, we found that the PEDF-knockout mice had an increased serum FSH level and an increased FSH/LH ratio, in view of this change and the reduction of the number of primordial follicles in PEDF-knockout mice, we confirmed that the PEDF-knockout mice showed DOR phenotype.

Recent studies have verified that ovarian oxidative damage is involved in ovarian aging, PCOS, DOR and other diseases [1,5]. In addition, the Nrf2 pathway, which is closely related to oxidative stress, is activated when oxidative stress occurs. Normally, the transcription factor Nrf2 is present in the cytoplasm and binds to kelch-like ech-

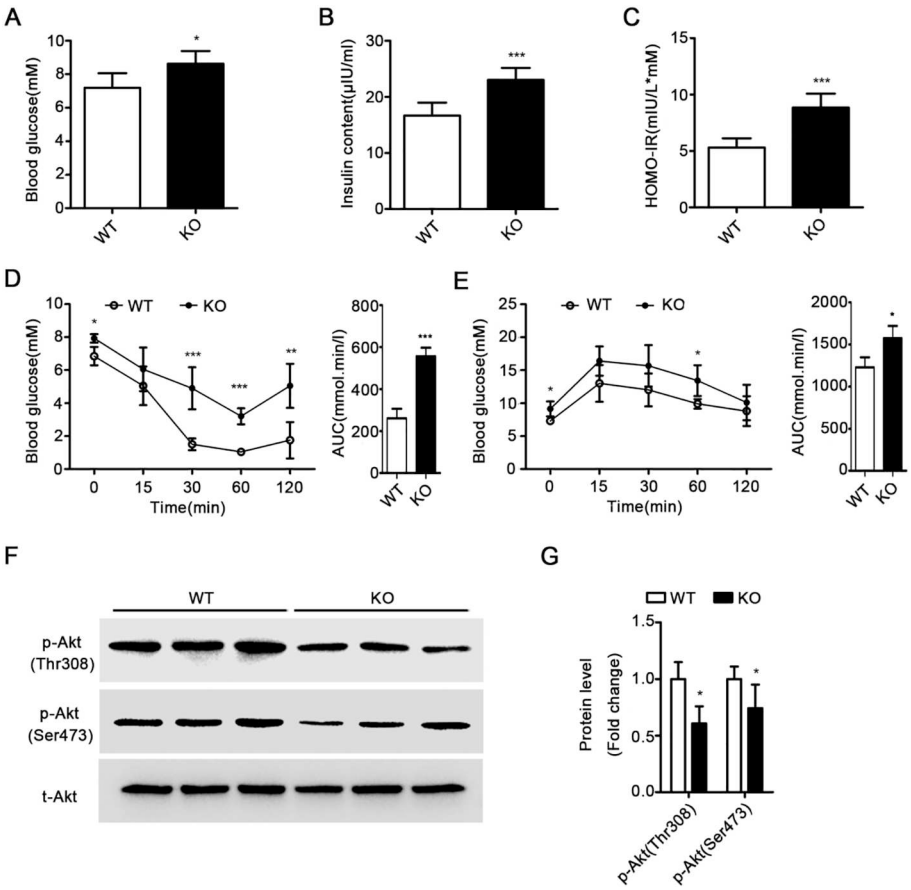

Fig. 7. Knockout of PEDF increased the blood glucose levels and induced hyperinsulinemia and insulin resistance. A. The fasting blood glucose levels of the mice. B. The serum fasting insulin contents of the mice. C. The HOMO-IR of the mice. D. The changes in the blood glucose levels in the ITT and the AUC of the ITT. E. The changes in the blood glucose levels in the GTT and the AUC of the GTT. F. The levels of the Akt pathway proteins in the mouse ovaries were detected by Western blotting. G. The fold changes of the levels of proteins related to the Akt pathway quantified based on the Western blotting results. Data are expressed as the mean ± SD. *, $p < 0.05$; **, $p < 0.01$; ***, $p < 0.001$.

associated protein-1 (Keap1). When oxidative stress occurs, SQSTM1 competitively occupies the Nrf2 binding site on Keap1 to prevent Nrf2 binding to Keap1 and leads to Nrf2 subsequent transfer into the nucleus; then, Nrf2 combines with antioxidant response element (ARE) and other antioxidant reaction elements to activate downstream antioxidant target genes, such as HO-1 and NQO1 [31]. In the present study, accumulation of ROS was found in the ovaries of the PEDF-knockout mice, and as expected, SQSTM1, nuclear Nrf2, HO-1, NQO1 and SOD1 expression was significantly increased in the ovaries of the PEDF-knockout mice compared to the levels in the wild-type mice. In addition, Aco, CYP2E1 and Nox2 play important roles in the generation of ROS [32]. In this study, we also found significant upregulation of Aco, CYP2E1 and Nox2. The results suggest that loss of PEDF can lead to severe oxidative stress in the mouse ovary, this may be the immediate cause of PEDF deficiency leading to ovarian damage.

In addition, an increasing number of studies have confirmed that an imbalance in the energy metabolism system plays a crucial role in some ovarian diseases [33–36]. For instance, lipotoxicity and insulin resistance often occur together and promote each other to jointly promote dysfunction of various tissues, including the ovaries [37–40]. Lipotoxicity refers to increased FFAs levels in the blood, which exceed the storage capacity of adipose tissue and the oxidative capacity of FFAs in tissues; this increase causes excess FFAs to be excessively deposited in non-fat tissues as TG, leading to tissue damage [41]. More importantly, excessive fatty acid oxidation leads to an increase in oxygen consumption that results in the accumulation of ROS and subsequent oxidative stress [42]. The ectopic deposition of fat and the excessive uptake of FFAs by tissues are key steps in lipotoxicity. Tissue lipotoxicity is an important feature of metabolic diseases and is widely found in patients with obesity, type 2 diabetes, metabolic syndrome, and non-alcoholic fatty liver [43–46]. Furthermore, increased levels of circulating FFAs or increased intracellular fat may affect the expression of genes related to the insulin pathway, such as Akt and forkhead box protein O1 (FOXO1), and induce and aggravate insulin resistance [40,47]. Insulin resistance refers to an inability of the organs to absorb and use glucose effectively due to decreased insulin sensitivity. When insulin resistance occurs, islet β cells secrete large amounts of insulin in a compensatory manner to maintain the blood glucose balance, leading to hyperinsulinemia. In turn, more severe insulin resistance will lead to higher levels of circulating FFAs in a vicious cycle [39,40].

Considering the close relationship between PEDF and lipid metabolism and the important role of energy metabolism imbalance in ovarian diseases, we evaluated the lipid metabolism of the PEDF-knockout mice. Lipid metabolic disorders were found in the PEDF-knockout mice that were mainly characterized by obesity, fat accumulation, severe ectopic fat deposition, and changes in the serum lipid and adipokine levels. As the body's largest metabolic organ, the liver plays a key role in the regulation of lipid metabolism in the body. When its metabolic function is impaired, the liver can cause lipid droplets to decompose, leading to a fatty liver. Importantly, the deposition of large amounts of lipid droplets in ovarian stromal cells suggests the presence of lipotoxicity in the ovary. TC, TG, FFAs, HDL, and LDL are the basic indexes for evaluating lipid metabolism. An excessive FFAs content in the peripheral blood is an important pathological factor leading to tissue lipotoxicity. When excessive FFAs in the peripheral blood exceed the storage or oxidizing capacity of the tissues, deposition of lipid droplets occurs. More critically, excessive fatty acid oxidation leads to an increase in oxygen consumption, resulting in the accumulation of ROS and subsequent oxidative stress. Additionally, adiponectin and leptin are important adipokines. Previous studies confirmed that elevated leptin levels had a significant negative effect on ovarian function and were associated with a number of diseases that affected pregnancy, such as PCOS, recurrent miscarriage, gestational diabetes mellitus, preeclampsia and intrauterine growth restriction [48,49]. Therefore, the

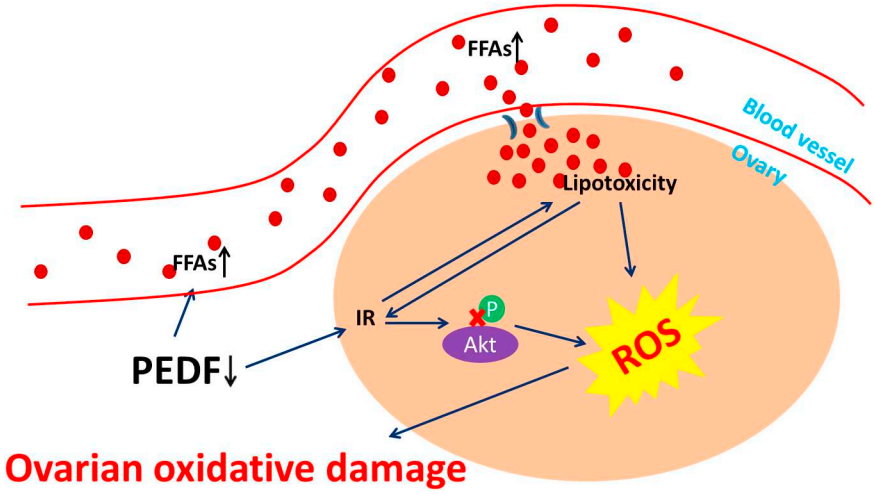

Fig. 8. A schematic diagram showing the role and mechanism of PEDF in ovarian oxidative damage. PEDF, pigment epithelium-derived factor; FFAs, free fatty acids; IR, insulin resistance; Akt, Protein kinase B; ROS, reactive oxygen species.

changes in serum adipokines and lipids suggest the occurrence of systemic disorders of lipid metabolism, which may be the key to ovarian oxidative damage. It is worth mentioning that although previous studies have shown a significant increase in serum PEDF levels in patients with various metabolic diseases including PCOS, our study suggests that the elevated circulating PEDF levels may be compensatory [16–21]. The present study suggests that the lipotoxicity caused by PEDF deficiency can lead to severe oxidative stress in the mouse ovary, this may be the primary cause of PEDF deficiency leading to ovarian damage.

As mentioned above, lipid metabolic disorders are often accompanied by insulin resistance, and both conditions constitute a vicious cycle [39,40]. Although the relationship between PEDF and insulin resistance is controversial, most previous studies have used the PEDF recombinant protein instead of knockout animals as the research tool [13,50–52]. Our results showed that PEDF knockout in female mice can lead to systemic insulin resistance. It should be emphasized that the controversy about the relationship between PEDF and insulin resistance is objective. We think the controversy over the relationship between PEDF and insulin resistance may be due to different research tools. Almost all of the previous studies supported the conclusion that PEDF can induce insulin resistance using PEDF recombinant protein as a research tool, while a few considered that PEDF can enhance insulin sensitivity using PEDF knockout or knockdown cells or animals, such as our study. [13,15,50–53] Obviously, the effects of endogenous PEDF or exogenous PEDF on insulin resistance may be quite different. As a secretory protein, PEDF is the most expressed in liver and fat [17,51]. Interestingly, liver and fat are highly insulin-sensitive tissues [51]. In previous studies, many of them increased circulating PEDF by recombinant protein treatment [13,50–52]. However, the effect of these methods on tissues PEDF levels and the dose-response relationship were neglected, which may be the underlying reason for the controversy over the relationship between PEDF and insulin resistance, but this needs further research to confirm. This study suggest that the insulin resistance caused by PEDF deficiency can aggravate lipotoxicity in the mouse ovary, this may be the another primary cause of PEDF deficiency leading to ovarian damage.

The key reason for insulin resistance is the phosphorylation of insulin receptor substrates 1(IRS1). Following phosphorylation of the IRS1, the Akt phosphorylation level significantly decreases [54]. The Akt pathway is closely related to glucose metabolism, lipid metabolism, and cell proliferation, differentiation and apoptosis, and its dysregulation can lead to a variety of diseases, including cancer, diabetes, and cardiovascular disease [54,55]. An increase in the Akt phosphorylation level is a hallmark of Akt pathway activation. Previous studies reported that a recombinant PEDF protein alleviated H_2O_2-induced oxidative damage in granulosa cells via a mechanism related to Akt phosphorylation [22]. Therefore, we examined the total and phosphorylated Akt levels in the ovaries of the PEDF-knockout mice and found that the Akt phosphorylation level was significantly reduced at both the Thr308 and Ser473 sites. This results further demonstrated the activation of Akt pathway by PEDF at the animal level. The Akt pathway may mediate the effect of PEDF against ovarian oxidative stress, but this speculation requires further proof.

5. Conclusion

In conclusion, we showed that loss of PEDF leads to ovarian oxidative damage accompanied by DOR in mice, this is related to PEDF deficiency induced severe insulin resistance and lipid metabolism disorder. PEDF deficiency affects ovarian function via multiple pathways. On the one hand, loss of PEDF results in high FFAs levels, leading to ovarian lipotoxicity and the induction of oxidative stress. On the other hand, PEDF deficiency induces insulin resistance, which in turn leads to dephosphorylation of Akt and thus oxidative stress. Insulin resistance and lipotoxicity promote each other, leading to the occurrence of ovarian oxidative damage (Fig. 8). Therefore, PEDF may be a potential target for the treatment of diseases related to ovarian oxidative damage.

Conflicts of interest

The authors declare no conflict of interest.

Author contributions

X.L. designed and performed the experiments, analyzed the data and wrote the manuscript. H.W. performed the histological staining experiment. J.T., Y.W. and M.Y. performed the QPCR experiment and provided useful advice on the manuscript and analyzed the data. C.M., S.G. and H.L. performed the controlled ovarian stimulation experiment. H.C. and W.C. designed the experiments and wrote the manuscript.

Acknowledgements

Funding: This research was funded by National Natural Science Foundation of China (Grant Number: 81670256, 81470015, 81741117, 81741017), Guangdong Science and Technology Department Project (Grant Number: 2016A020216005, 2015B090903063, 2015A020212006), and Guangzhou Science and Technology Program key projects (Grant Number: 201510010052). The funders had no role in study design, data collection and analysis, decision to publish, or preparation of the manuscript.

We also thank Dr. Guoquan Gao (Zhongshan School of Medicine, Sun Yat-sen University) for providing the PEDF-knockout mice.

References

[1] J. Wojsiat, J. Korczynski, M. Borowiecka, et al., The role of oxidative stress in female infertility and in vitro fertilization, Postepy Hig. Med. Dosw. 71 (2017) 359–366.
[2] P.J. Devine, S.D. Perreault, U. Luderer, Roles of reactive oxygen species and antioxidants in ovarian toxicity, Biol. Reprod. 86 (2012) 27.
[3] J. Lim, U. Luderer, Oxidative damage increases and antioxidant gene expression decreases with aging in the mouse ovary, Biol. Reprod. 84 (2011) 775–782.
[4] J. Lim, B.N. Nakamura, I. Mohar, et al., Glutamate cysteine ligase modifier subunit (Gclm) null mice have increased ovarian oxidative stress and accelerated age-related ovarian failure, Endocrinology 156 (2015) 3329–3343.
[5] A.K. Pandey, A. Gupta, M. Tiwari, et al., Impact of stress on female reproductive health disorders: possible beneficial effects of shatavari (*Asparagus racemosus*), Biomed. Pharmacother. 103 (2018) 46–49.
[6] J. Tombran-Tink, K. Mazuruk, I.R. Rodriguez, et al., Organization, evolutionary conservation, expression and unusual Alu density of the human gene for pigment epithelium-derived factor, a unique neurotrophic serpin, Mol. Vis. 2 (1996) 11.
[7] E. Stratikos, E. Alberdi, P.G. Gettins, et al., Recombinant human pigment epithelium-derived factor (PEDF): characterization of PEDF overexpressed and secreted by eukaryotic cells, Protein Sci. 5 (1996) 2575–2582.
[8] D. Chuderland, I. Ben-Ami, H. Bar-Joseph, et al., Role of pigment epithelium-derived factor in the reproductive system, Reproduction 148 (2014) R53–R61.
[9] C. Kampfer, S. Saller, S. Windschuttl, et al., Pigment-Epithelium Derived Factor (PEDF) and the human ovary: a role in the generation of ROS in granulosa cells, Life Sci. 97 (2014) 129–136.
[10] S. Yamagishi, T. Matsui, Pigment epithelium-derived factor (PEDF) and cardiometabolic disorders, Curr. Pharm. Des. 20 (2014) 2377–2386.
[11] M.M. Bilak, A.M. Corse, S.R. Bilak, et al., Pigment epithelium-derived factor (PEDF) protects motor neurons from chronic glutamate-mediated neurodegeneration, J. Neuropathol. Exp. Neurol. 58 (1999) 719–728.
[12] T. Falk, R.T. Gonzalez, S.J. Sherman, The Yin and Yang of VEGF and PEDF: multifaceted neurotrophic factors and their potential in the treatment of Parkinson's disease, Int. J. Mol. Sci. 11 (2010) 2875–2900.
[13] S. Crowe, L.E. Wu, C. Economou, et al., Pigment epithelium-derived factor contributes to insulin resistance in obesity, Cell Metab. 10 (2009) 40–47.
[14] T.V. Lakeland, M.L. Borg, M. Matzaris, et al., Augmented expression and secretion of adipose-derived pigment epithelium-derived factor does not alter local angiogenesis or contribute to the development of systemic metabolic derangements, Am. J. Physiol. Endocrinol. Metab. 306 (2014) E1367–E1377.
[15] T. Matsui, Y. Nishino, A. Ojima, et al., Pigment epithelium-derived factor improves metabolic derangements and ameliorates dysregulation of adipocytokines in obese type 2 diabetic rats, Am. J. Pathol. 184 (2014) 1094–1103.
[16] C. Chen, A.W. Tso, L.S. Law, et al., Plasma level of pigment epithelium-derived factor is independently associated with the development of the metabolic syndrome in Chinese men: a 10-year prospective study, J. Clin. Endocrinol. Metab. 95 (2010) 5074–5081.
[17] Z. Dai, W. Qi, C. Li, et al., Dual regulation of adipose triglyceride lipase by pigment epithelium-derived factor: a novel mechanistic insight into progressive obesity, Mol. Cell. Endocrinol. 377 (2013) 123–134.
[18] Z. Dai, T. Zhou, C. Li, et al., Intracellular pigment epithelium-derived factor contributes to triglyceride degradation, Int. J. Biochem. Cell Biol. 45 (2013) 2076–2086.
[19] A. Jenkins, S.X. Zhang, A. Gosmanova, et al., Increased serum pigment epithelium derived factor levels in Type 2 diabetes patients, Diabetes Res. Clin. Pract. 82 (2008) e5–e7.
[20] M. Sabater, J.M. Moreno-Navarrete, F.J. Ortega, et al., Circulating pigment epithelium-derived factor levels are associated with insulin resistance and decrease after weight loss, J. Clin. Endocrinol. Metab. 95 (2010) 4720–4728.
[21] S. Yang, Q. Li, L. Zhong, et al., Serum pigment epithelium-derived factor is elevated in women with polycystic ovary syndrome and correlates with insulin resistance, J. Clin. Endocrinol. Metab. 96 (2011) 831–836.
[22] H. Bar-Joseph, I. Ben-Ami, R. Ron-El, et al., Pigment epithelium-derived factor exerts antioxidative effects in granulosa cells, Fertil. Steril. 102 (2014) 891–898 (e893).
[23] W. Zhuang, H. Zhang, J. Pan, et al., PEDF and PEDF-derived peptide 44mer inhibit oxygen-glucose deprivation-induced oxidative stress through upregulating PPARgamma via PEDF-R in H9c2 cells, Biochem. Biophys. Res. Commun. 472 (2016) 482–488.
[24] S. Yamagishi, T. Matsui, K. Nakamura, et al., Pigment-epithelium-derived factor (PEDF) inhibits angiotensin-II-induced vascular endothelial growth factor (VEGF) expression in MOLT-3 T cells through anti-oxidative properties, Microvasc. Res. 71 (2006) 222–226.
[25] Yamagishi S-i, K. Nakamura, S. Ueda, et al., Pigment epithelium-derived factor (PEDF) blocks angiotensin II signaling in endothelial cells via suppression of NADPH oxidase: a novel anti-oxidative mechanism of PEDF, Cell Tissue Res. 320 (2005) 437–445.
[26] S.X. Zhang, J.J. Wang, A. Dashti, et al., Pigment epithelium-derived factor mitigates inflammation and oxidative stress in retinal pericytes exposed to oxidized low-density lipoprotein, J. Mol. Endocrinol. 41 (2008) 135–143.
[27] A.K. Champlin, D.L. Dorr, A.H. Gates, Determining the stage of the estrous cycle in the mouse by the appearance of the vagina, Biol. Reprod. 8 (1973) 491–494.
[28] C.E. Aiken, J.L. Tarry-Adkins, N.C. Penfold, et al., Decreased ovarian reserve, dysregulation of mitochondrial biogenesis, and increased lipid peroxidation in female mouse offspring exposed to an obesogenic maternal diet, FASEB J. 30 (2016) 1548–1556.
[29] Z. Jamil, S.S. Fatima, K. Ahmed, et al., Anti-Mullerian hormone: above and beyond conventional ovarian reserve markers, Dis. Markers 2016 (2016) 5246217.
[30] J.S. Younis, J.E. Jadaon, S. Haddad, et al., Prospective evaluation of basal stromal Doppler studies in women with good ovarian reserve and infertility undergoing in vitro fertilization-embryo transfer treatment: patients with polycystic ovary syndrome versus ovulatory patients, Fertil. Steril. 95 (2011) 1754–1758.
[31] I. Buendia, P. Michalska, E. Navarro, et al., Nrf2-ARE pathway: an emerging target against oxidative stress and neuroinflammation in neurodegenerative diseases, Pharmacol. Ther. 157 (2016) 84–104.
[32] D. Ye, Y. Wang, H. Li, et al., Fibroblast growth factor 21 protects against acetaminophen-induced hepatotoxicity by potentiating peroxisome proliferator-activated receptor coactivator protein-1alpha-mediated antioxidant capacity in mice, Hepatology 60 (2014) 977–989.
[33] Q.N. Di, W.X. Cao, R. Xu, et al., Chronic low-dose exposure of nonylphenol alters energy homeostasis in the reproductive system of female rats, Toxicol. Appl. Pharmacol. 348 (2018) 67–75.
[34] R. Huang, X. Xue, S. Li, et al., Alterations of polyunsaturated fatty acid metabolism in ovarian tissues of polycystic ovary syndrome rats, J. Cell. Mol. Med. 22 (7) (2018) 3388–3396.
[35] Y. Wu, Y. Li, X. Liao, et al., Diabetes induces abnormal ovarian function via triggering apoptosis of granulosa cells and suppressing ovarian angiogenesis, Int. J. Biol. Sci. 13 (2017) 1297–1308.
[36] P.C. Leung, J. Wang, The role of inositol lipid metabolism in the ovary, Biol. Reprod. 40 (1989) 703–708.
[37] Q.Q. Tang, Lipid metabolism and diseases, Sci. Bull. 61 (2016) 1471–1472.
[38] A. Fernandez-Sanchez, E. Madrigal-Santillan, M. Bautista, et al., Inflammation, oxidative stress, and obesity, Int. J. Mol. Sci. 12 (2011) 3117–3132.
[39] S.M. Alwahsh, B.J. Dwyer, S. Forbes, et al., Insulin production and resistance in different models of diet-induced obesity and metabolic syndrome, Int. J. Mol. Sci. 18 (2017).
[40] G. Boden, Obesity, insulin resistance and free fatty acids, Curr. Opin. Endocrinol. Diabetes Obes. 18 (2011) 139–143.
[41] N.A. van Herpen, V.B. Schrauwen-Hinderling, Lipid accumulation in non-adipose tissue and lipotoxicity, Physiol. Behav. 94 (2008) 231–241.
[42] A.H. de Mello, A.B. Costa, J.D.G. Engel, et al., Mitochondrial dysfunction in obesity, Life Sci. 192 (2018) 26–32.
[43] Q. Chen, M. Liu, H. Yu, et al., *Scutellaria baicalensis* regulates FFA metabolism to ameliorate NAFLD through the AMPK-mediated SREBP signaling pathway, J. Nat. Med. 72 (3) (2018) 655–666.
[44] D.J. Hodson, R.K. Mitchell, E.A. Bellomo, et al., Lipotoxicity disrupts incretin-regulated human beta cell connectivity, J. Clin. Invest. 123 (2013) 4182–4194.
[45] D. Petrakis, L. Vassilopoulou, C. Mamoulakis, et al., Endocrine disruptors leading to obesity and related diseases, Int. J. Environ. Res. Public Health 14 (2017).
[46] M. Zhou, R.M. Learned, S.J. Rossi, et al., Engineered FGF19 eliminates bile acid toxicity and lipotoxicity leading to resolution of steatohepatitis and fibrosis in mice, Int. Hepatol. Commun. 1 (2017) 1024–1042.
[47] N. Stefan, H.U. Haring, Circulating fetuin-A and free fatty acids interact to predict insulin resistance in humans, Nat. Med. 19 (2013) 394–395.
[48] A. Perez-Perez, A. Toro, T. Vilarino-Garcia, et al., Leptin action in normal and pathological pregnancies, J. Cell. Mol. Med. 22 (2018) 716–727.
[49] S.F. Li, X. Li, Leptin in normal physiology and leptin resistance, Sci. Bull. 61 (2016) 1480–1488.
[50] S. Famulla, D. Lamers, S. Hartwig, et al., Pigment epithelium-derived factor (PEDF) is one of the most abundant proteins secreted by human adipocytes and induces insulin resistance and inflammatory signaling in muscle and fat cells, Int. J. Obes. 35 (2011) 762–772.
[51] R. Carnagarin, A.M. Dharmarajan, C.R. Dass, PEDF attenuates insulin-dependent molecular pathways of glucose homeostasis in skeletal myocytes, Mol. Cell. Endocrinol. 422 (2016) 115–124.
[52] M.L. Borg, Z.B. Andrews, E.J. Duh, et al., Pigment epithelium-derived factor

regulates lipid metabolism via adipose triglyceride lipase, Diabetes 60 (2011) 1458–1466.
[53] A.K. Gattu, A.L. Birkenfeld, Y. Iwakiri, et al., Pigment epithelium-derived factor (PEDF) suppresses IL-1beta-mediated c-Jun N-terminal kinase (JNK) activation to improve hepatocyte insulin signaling, Endocrinology 155 (2014) 1373–1385.
[54] I. Hers, E.E. Vincent, J.M. Tavare, Akt signalling in health and disease, Cell. Signal. 23 (2011) 1515–1527.
[55] M.A. Hermida, J. Dinesh Kumar, N.R. Leslie, GSK3 and its interactions with the PI3K/AKT/mTOR signalling network, Adv Biol Regul 65 (2017) 5–15.